

# Experimental Cross Sections And Velocities Of Light Nuclides Produced In The Proton-Induced Fission Of $^{238}\text{U}$ At 1 GeV

*M. V. Ricciardi<sup>a</sup>, K. -H. Schmidt<sup>a</sup>, F. Rejmund<sup>a</sup>, T. Enqvist<sup>a</sup>,  
P. Armbruster<sup>a</sup>, J. Benlliure<sup>b</sup>, M. Bernas<sup>c</sup>, B. Mustapha<sup>c</sup>, L. Tassan-Got<sup>c</sup>,  
C. Stephan<sup>d</sup>, A. Boudard<sup>d</sup>, S. Leray<sup>d</sup>, C. Volant<sup>d</sup>, S. Czajkowski<sup>e</sup>,  
M. Pravikoff<sup>e</sup>*

<sup>a</sup>GSI, Planckstr. 1, D-64291 Darmstadt, Germany

<sup>b</sup>Universidad de Santiago de Compostela, Dpto. de Fisica, E-15706, Spain

<sup>c</sup>IPN Orsay, IN2P3, F-91406 Orsay, France

<sup>d</sup>CEA Saclay, F-91191 Gif sur Yvette, France

<sup>e</sup>CEN Bordeaux-Gradignan, F-33175 Gradignan, France

**Abstract.** Light nuclides produced in collisions of 1 A GeV  $^{238}\text{U}$  with hydrogen have been observed with a high-resolution forward magnetic spectrometer, the fragment separator (FRS), at GSI. Fragments were identified in  $A$  and  $Z$  and their production cross-sections measured. For each nuclide the velocity was precisely determined from the measured magnetic rigidity. This insight into the kinematics of the relativistic nuclear collisions allowed disentangling different reaction mechanisms. Thanks to the combined results on  $A$ ,  $Z$ , and velocity of the fragments it was found out that all the observed isotopes, from  $Z=37$  down to the last element measured ( $Z=7$ ), were formed in a binary decay process, interpreted as fission. A qualitative analysis of the cross sections revealed that the charge distribution of these light fragments, which forms a plateau around  $Z=15$  and increases below  $Z=13$ , is in agreement with the theoretical expectations of the statistical model.

**Keywords:** Nuclear fission; light fission fragments; IMF emission; statistical model.

**PACS:** 25.85.-w; 25.85.Ge; 24.60.Dr; 21.10.Ft; 21.10.Gv.

## INTRODUCTION

In 1996, at GSI, Darmstadt, a European collaboration started a dedicated experimental program, devoted to reaching a full comprehension of the proton-induced spallation reactions in the energy range 0.3-1.5 GeV per nucleon. Within this project, the systems  $^{56}\text{Fe} + ^{1,2}\text{H}$ ,  $^{136}\text{Xe} + ^1\text{H}$ ,  $^{197}\text{Au} + ^1\text{H}$ ,  $^{208}\text{Pb} + ^{1,2}\text{H}$  and  $^{238}\text{U} + ^{1,2}\text{H}$  have been studied. The study of light-residue production (from  $Z=7$  to  $Z=37$ ) in hydrogen-induced reactions of  $^{238}\text{U}$  presented here belongs to this systematic study. Together with three other investigations which proceeded in parallel and which are dedicated to the formation of heavier residues by fission<sup>1</sup> (from  $Z=28$  to  $Z=73$ ) and by fragmentation<sup>2</sup> (from  $Z=74$  to  $Z=92$ ) in the system  $^{238}\text{U} + \text{hydrogen}$ , the whole chart of the nuclides from  $Z=7$  on is covered. An overview of all the results for the reaction  $^{238}\text{U}$  on hydrogen at 1 A GeV are given in a dedicated letter<sup>3</sup>. In the reaction  $^{238}\text{U} +$

hydrogen at 1  $A$  GeV, apart from spallation reactions, which end up in rather heavy fragments (see ref. 2 and also the contribution of M. Bernas to this workshop), most part of the cross sections of the medium-mass residues results from fission reactions. One of the most important signatures of fission is the binary nature of the decay process. The light residues, investigated in this work, also show a binary nature. However, binary decay can occur also via multifragmentation, which is the process responsible for the production of light nuclei in most high-energy nuclear reactions. The possible scenarios behind fission and multifragmentation are indeed strongly different, because the first presupposes the slow decay of a compound nucleus, while the second one the passage through a fast break-up phase. In this work, we will discuss whether the light residues that we observed are consistent with scenario of a binary decay of a compound nucleus, namely, fission.

## THE EXPERIMENT

The experiment was performed with a high-resolution, forward, two-stage magnetic spectrometer, the fragment separator (FRS), at GSI. The primary beam of  $^{238}\text{U}$ , at the energy of 1  $A$  GeV, impinged on a liquid-hydrogen target, placed inside a titanium container at the entrance of the FRS. The primary-beam intensity was constantly monitored. The fragments produced in the interaction of the beam with the target were detected at the exit of the FRS. The equipment along the FRS consisted mainly of two scintillators, placed at the intermediate image plane and at the exit, and of an ionisation chamber, placed behind the FRS. The ionisation chamber recorded the energy loss of the produced ions, and from that, the nuclear charge of the reaction products was deduced. The two scintillation detectors were used to detect the horizontal positions as well as the time-of-flight between the mid-plane and the exit. The combined information on positions at mid- and final-image-plane and velocity (measured by the time-of-flight) gave a measurement of the magnetic rigidity ( $B\rho$ ) of the ion passing through the FRS. According to the equation:

$$B\rho = \frac{A \cdot \gamma \cdot v \cdot m_0}{Z \cdot e} \quad (1)$$

(where  $v$  is the velocity of the ion,  $\gamma$  is the relativistic parameter,  $m_0$  the nuclear mass unit, and  $e$  the charge of an electron), the mass number  $A$  of any reaction product could be determined once the nuclear charge  $Z$  was determined. The full identification was possible for every produced nuclide, thanks to high resolving power in  $Z$  and  $A$  ( $Z/\Delta Z = 150$ ,  $A/\Delta A = 400$ ). Once every produced nuclide was identified (thus its mass  $A$  and charge  $Z$  were integer numbers), its velocity could easily be calculated from equation (1) with an accuracy that depends only on  $B\rho$ . This method gives an absolute measurement of the velocity, which does not suffer from calibration problems and produces a very accurate result, being the resolution in magnetic rigidity about  $3 \cdot 10^{-4}$ .

Due to the limited momentum acceptance of the FRS it was necessary to combine several measurements with fixed  $B\rho$  in order to cover all  $A/Z$  and velocities. Once this was done, it was possible to reconstruct the two-dimensional cluster-plot of the

velocity distribution as a function of the neutron number for every element. In Figure 1-right, the velocity of iron isotopes produced in fission and fragmentation reactions is presented in the beam frame. Every vertical line represents the velocity distribution of one isotope. The pictures must be observed keeping in mind the limited angular acceptance of the spectrometer, represented by the cone of Figure 1-left, which produced the characteristic triple-humped velocity distributions: fragments distributed in the central part of the spectrum come from the fragmentation reactions, while those with higher positive and negative velocities are produced in fission events. The spectrum in the Figure 1-right collects the counts from the hydrogen target, including a contribution from the titanium windows. From the comparison with data taken with a thin titanium target of the same thickness of the windows of the container, we deduced that the nuclei with the extreme velocity values (fission fragments) are mostly due to the interaction of uranium with protons, while the central part (fragmentation products) is mostly due to the interaction of uranium with titanium.

The recoil velocity of the fissioning nuclei could be determined from the difference of the mean positions of the two external peaks of the velocity spectrum. From this knowledge, the mean velocity of the fission fragments in the fissioning-nucleus frame could be determined too.

From the integral of the three different components of the velocity spectrum, knowing the beam intensities, the target properties and the ratios of the transmitted reaction residues (which can be calculated), the production cross sections were determined both for fission and for fragmentation products.

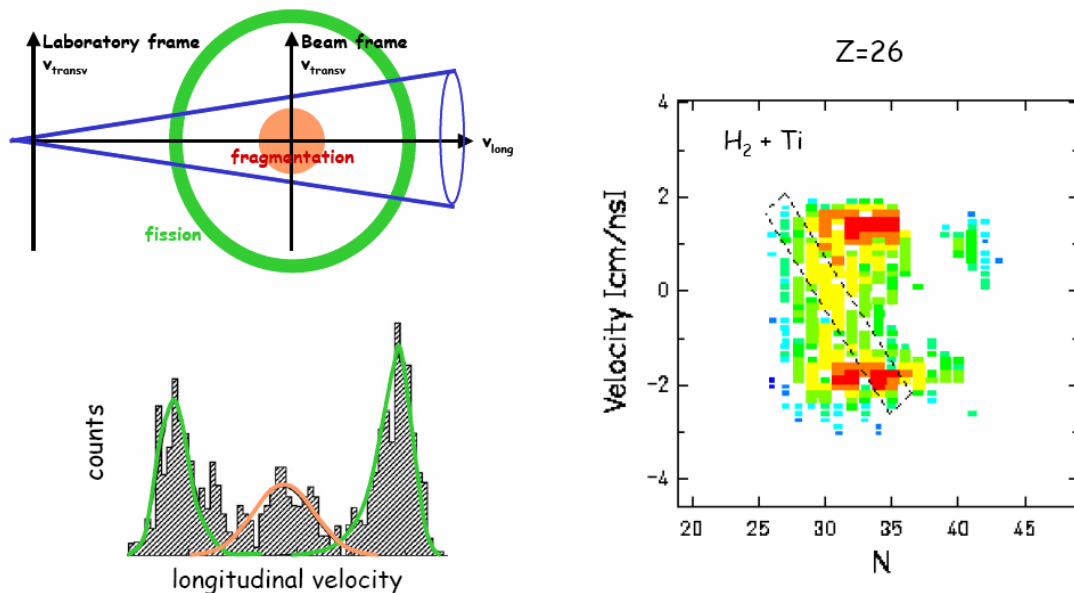


**FIGURE 1.** Left: Schematic representation of the limited angular acceptance of the FRS, which produces the characteristic triple-humped velocity distribution of the fission and fragmentation products. Right: Longitudinal velocity of iron isotopes produced in fission and fragmentation reactions, presented in the beam frame (the zero of the y axis represents the velocity of the beam).

## INTERPRETATION OF THE EXPERIMENTAL RESULTS

### Velocity of the fission fragments

The mean velocity of fission fragments can be estimated by the following empirical liquid-drop description of the total kinetic energy:

$$TKE = \frac{Z_1 Z_2 e^2}{D} \quad \text{with} \quad D = r_0 A_1^{1/3} \left( 1 + \frac{2\beta_1}{3} \right) + r_0 A_2^{1/3} \left( 1 + \frac{2\beta_2}{3} \right) + d \quad (2)$$

where  $A_1, A_2, Z_1, Z_2$  denote the mass and charge numbers of a pair of fission fragments prior to neutron evaporation.  $D$  represents the distance between the two charges and is given by the fragment radii ( $r_0 A^{1/3}$ ), corrected for the deformation ( $\beta$ ), plus the neck ( $d$ ). The parameters ( $r_0=1.16$  fm,  $d=2.0$  fm,  $\beta_1=\beta_2=0.625$ ) were deduced from experimental data in ref. 4. The formula (2) is valid for sufficiently excited nuclei, where shell effects are negligible. When the momentum conservation is imposed to the reaction, the velocities of the two fission fragments are determined.

We have estimated the mean velocities of the fission fragments for two compound nuclei:  $^{238}\text{U}$  and  $^{185}\text{Au}$ . They are compared with the experimental data in Figure 2 (for technical reasons, the mean velocity could not be determined for fragments below  $Z=17$ ). While for the heavier fragments, the experimental data fall in between these two estimates, for fragments below  $Z = 25$ , the mean velocity tends to be higher than the estimation for the  $^{238}\text{U}$  compound nucleus. This is due to the fact that the experimental parameters of equation (2) that were obtained in symmetric fission are not applicable to very asymmetric mass splits. In very asymmetric fission, both the neck (parameter  $d$ ) and the deformation (parameter  $\beta$ ) might be smaller, with a consequent increase of the kinetic energy.

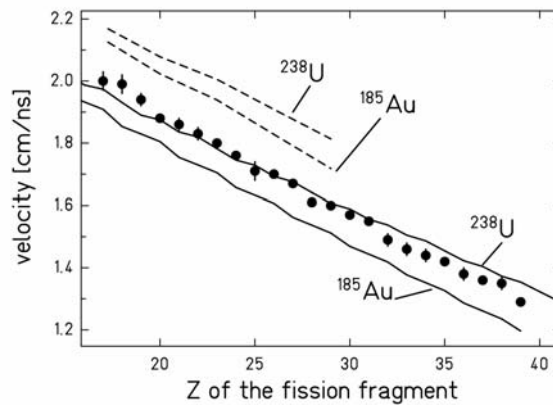


**FIGURE 2.** Measured mean values of the velocities of fission fragments in the frame of the fissioning nucleus ( $\bullet$ ). The lines represent the expected values of the velocity of fragments originating from the compound nuclei  $^{238}\text{U}$  and  $^{185}\text{Au}$ . The solid lines represent the expected velocities for the scission-point model (deformed nuclei) and the dashed lines the values obtained by the nucleus-nucleus fusion approach (undeformed nuclei).

To verify the validity of this assumption, we have performed a calculation of the mean velocity in case of asymmetric binary decay from undeformed nuclei. We assumed that the binary decay can be described as the inverse process of fusion. The shape of the potential is given in terms of the nuclear, Coulomb and centrifugal contributions. In our calculations, the empirical nuclear potential of R.Bass<sup>5</sup> was used. The total kinetic energy of the two nuclei is assumed to be equal to the height of the potential barrier. Imposing momentum conservation, the velocity of the two fragments was determined. The result of this calculation for the compound nuclei <sup>238</sup>U and <sup>185</sup>Au is represented in Figure 2 by the dashed lines. The experimental data fall in between the cases of a split into highly deformed nuclei and undeformed nuclei.

This result gives an indication that the lightest fragments are produced in configurations which are more compact than predicted by the systematics of equation (2) that is based on more symmetric fission. We take this fact as an indication of the transition from fission to the evaporation of intermediate-mass fragments.

## Cross sections

In Figure 3-right the production cross sections of the fission fragments are presented in form of charge distribution. The Figure includes the heavier fragments obtained in the parallel analysis<sup>1,2</sup>. Please note that our measurement was technically limited to  $Z \geq 7$ , but the production of light nuclides would extend even farther down to  $Z=1$ . One can notice that, as expected, the cross sections are very high in the main fission region and decrease rapidly from  $Z=30$  to  $Z=20$ . But then they stay constant and finally slightly increase again below  $Z=10$ .

The observed change of slope of the charge distribution can be explained by means of the statistical model. Figure 3 includes also the prediction obtained with a statistical code obtained combining the output results of the intranuclear cascade stage predicted by INCL3<sup>6</sup> with the deexcitation stage ABLA<sup>7,8</sup>. ABLA is a statistical model where the compound nucleus at every step of its evolution has two possible decay channels: evaporation and fission. Evaporation is treated as described in ref. 7 and fission as described in ref. 8. In the statistical model of fission for a given excitation energy the yield of a certain fission fragment is determined by the statistical weight of the transition states above the potential barrier, i.e. at the saddle point. This weight is in turn correlated to the density of nuclear levels. In ABLA, the latter are calculated using the thermodynamic Fermi-gas picture, i.e. assuming the nucleus as a system of non-interacting fermionic particles. The potential energy at the saddle-point depends on mass-asymmetric deformations, which lead to the formation of two fragments of different sizes. In the fission model of ABLA, the barrier as a function of mass asymmetry is defined by three components. The first is the symmetric component defined by the liquid-drop potential by means of a parabolic function with a curvature obtained from experimental data<sup>9</sup>. This parabola is modulated by two neutron shells, represented by Gaussian functions. Shells are supposed to wash out with excitation energy<sup>10</sup>. The heights and the widths of the Gaussians representing the shell effects and additional fluctuations in mass asymmetry acquired from saddle to scission are derived from experimental data. The above representation of the barrier as a function of mass asymmetry is valid only for the main fission region (from  $Z=20$  to  $Z=65$

approximately), while for very asymmetric mass splits the potential energy is expected to inverse the slope and start to decrease. This aspect has been widely discussed in the past in terms of “conditional saddle”<sup>11</sup>. From the physical point of view an extremely asymmetric binary split corresponds to an evaporation of a light nucleus. Up to now the evaporation part of ABLA considered only the emission of light particles, specifically: neutrons, protons, tritons, deuterons, <sup>3</sup>He and alphas. We implemented in the code the evaporation of intermediate-mass fragments (IMF), i.e. light nuclei with  $Z > 2$ . The statistical weight for the emission of these fragments is calculated on the basis of the detailed-balance principle, and depends mostly on the ratio of the level density of the nuclear system at the barrier and the level density of the compound nucleus (at ground state). The barrier is calculated using the fusion nuclear potential of Bass.

In Figure 3 the result of the code is presented in form of chart of the nuclides (left) and of charge distribution (right). The latter result is compared with the experimental data. The full line is obtained by the sum of the three components: the evaporated IMF, the fission fragments and the evaporation residues.

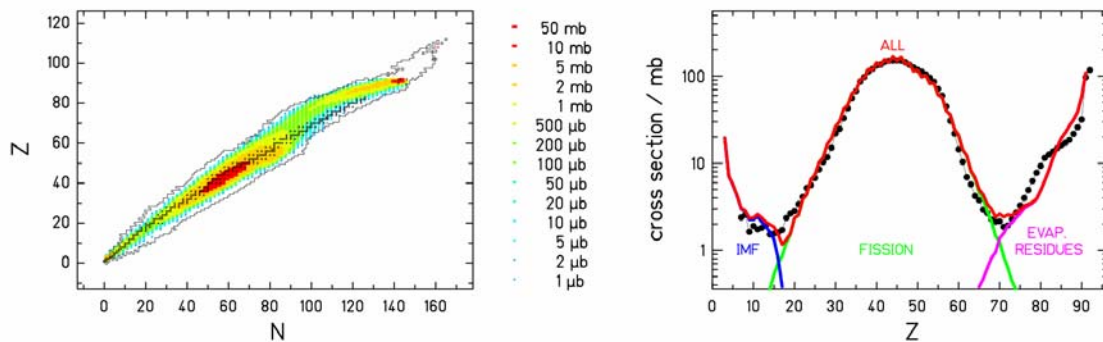


**FIGURE 3.** Production cross-sections for the reaction  $^{238}\text{U}$  (1.4 GeV) + p. Left: Prediction of INCL+ABLA presented on the chart of the nuclides. Right: Experimental data (full dots) are compared with the results of INCL+ABLA.

In Figure 4, the isotopic distributions of the first eight measured elements are compared with the prediction of INCL+ABLA. The agreement is extremely good. Results for the mean values of the isotopic distributions of every element are summarised in Figure 5. There, the mean  $N/Z$ -ratio is shown as a function of the proton number. The solid line is the result of the INCL+ABLA prediction. In the fission model inside ABLA, the population of the fission channels is assumed to be basically determined by the statistical weight of transition states above the potential-energy landscape at the fission barrier, as described previously. Several properties, however, are finally determined at scission, among them the mean value and the fluctuations in the neutron-to-proton ratio, which are responsible for the so-called “charge polarisation”. It can be noticed that the calculation reproduces rather well the mean values (the  $\langle N \rangle / Z$ -ratio) of the isotopic distributions. This is an indication that both the charge polarisation in the fission process and the competition with the evaporation of neutrons in the statistical model are rather well described in the code.

The lightest products are neutron rich, as expected to be in fission. Compared to electromagnetic-induced fission, where the mean  $N/Z$  is close to that one of  $^{238}\text{U}$ , here the neutron excess is lower, demonstrating that the process occurred at higher excitation energies. The neutron enrichment decreases slightly with the decreasing mass. The reason for this tendency is connected to the fact that the valley of stability becomes quickly narrow and steep. Large fluctuations in  $N/Z$  become more and more unlikely.

To conclude this section, we like to point out that the result of the ABLA code is remarkable, because the theoretical model behind it could never be compared before with experimental results on fully identified nuclide distributions in the region of light fission fragments from proton-induced fission.

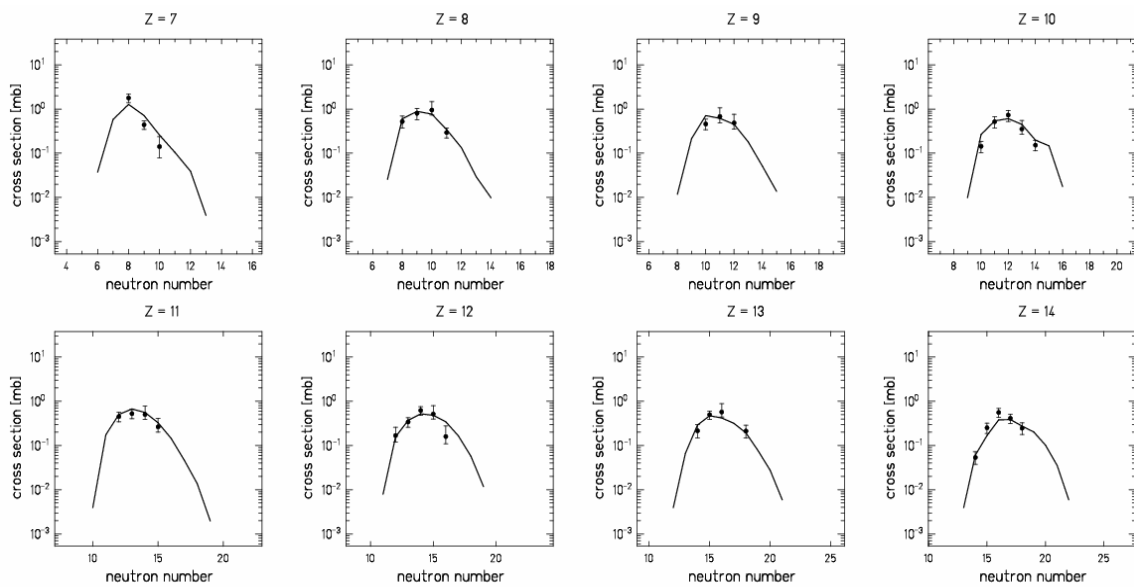


**FIGURE 4.** Cross sections for the isotopes of the eighth lightest elements measured in the reaction  $^{238}\text{U}$  (1-A GeV) + p. The solid line represents the prediction of INCL+ABLA.

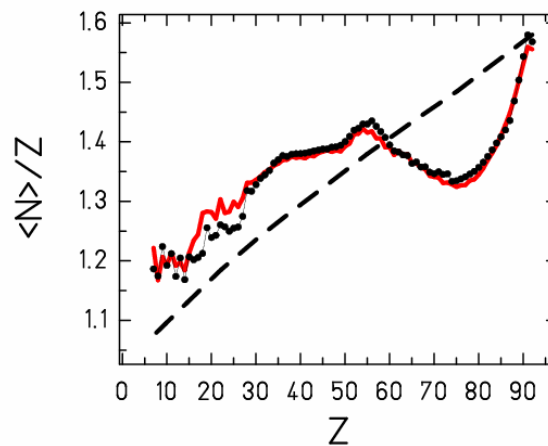


**FIGURE 5.** Mean neutron-to-proton ratio of isotopic distributions as a function of the atomic number. The experimental data (dots) are compared to the the prediction of the INCL+ABLA code (full line) and to the stability line (dashed line).

## CONCLUSIONS

Despite the long study of fission, there is still very little experimental information available on the light residues produced in very asymmetric fission of actinides. Here, 254 light residues in the element range  $7 \leq Z \leq 37$  formed in the proton-induced reactions of  $^{238}\text{U}$  at 1 A GeV were presented. This experimental work belongs to a systematic study of the reaction  $^{238}\text{U} + ^1\text{H}$  at 1 A GeV, where the production of nuclides with  $7 \leq Z \leq 92$  was measured and analysed. The other experimental data, complementing those presented here, can be found in refs. 1, 2, 3.

The light fragments presented here, which populate the chart of the nuclides far down, could be qualified as binary-decay products thanks to the available kinematic information. The study of all the experimental observables, the production cross sections and the velocities, showed that these signatures are consistent with the binary decay of a fully equilibrated compound nucleus. As discussed in ref. 11, the binary decay of a compound nucleus includes fission and evaporation with a natural transition in-between, and it might be called fission in a generalized sense. Thus, very asymmetric fission of the system  $^{238}\text{U} + ^1\text{H}$  at 1 A GeV seems to reach down to rather light nuclei, extending below  $Z = 7$ . In the spallation-fission reaction of  $^{238}\text{U}$  this feature is unambiguously identified for the first time. The production cross sections could be satisfactorily reproduced by a statistical model.

## ACKNOWLEDGMENTS

The work has been supported by the European Community with the programmes under the contracts: ERBCHB CT 94 0717, HPRI 1999 CT 00001, FIKW CT 2000 00031, and HPRI-1999-CT-50001.

## REFERENCES

- 1 M. Bernas, P. Armbruster, J. Benlliure, A. Boudard, E. Casarejos, S. Czajkowski, T. Enqvist, R. Legrain, S. Leray, B. Mustapha, P. Napolitani, J. Pereira, F. Rejmund, M.-V. Ricciardi, K.-H. Schmidt, C. Stéphan, J. Taïeb, L. Tassan-Got, and C. Volant, *Nucl. Phys. A* **725**, 213-253 (2003).
- 2 J. Taïeb, K.-H. Schmidt, L. Tassan-Got, P. Armbruster, J. Benlliure, M. Bernas, A. Boudard, E. Casarejos, S. Czajkowski, T. Enqvist, R. Legrain, S. Leray, B. Mustapha, M. Pravikoff, F. Rejmund, C. Stéphan, C. Volant and W. Wlazło, *Nucl. Phys. A* **724**, 413-430 (2003).
- 3 P. Armbruster, J. Benlliure, M. Bernas, A. Boudard, E. Casarejos, S. Czajkowski, T. Enqvist, S. Leray, P. Napolitani, J. Pereira, F. Rejmund, M. V. Ricciardi, K.-H. Schmidt, C. Stéphan, J. Taïeb, L. Tassan-Got and C. Volant, *Phys. Rev. Lett.* **93**, 212701 (2004).
- 4 C. Böckstiegel, S. Steinhäuser, J. Benlliure, H.-G. Clerc, A. Grewe, A. Heinz, M. de Jong, A.R. Junghans, J. Müller and K.-H. Schmidt, *Phys. Lett. B* **398** 259-267 (1997).
- 5 R. Bass, Proceeding of the Symposium on Deep-Inelastic and Fusion Reactions with Heavy Ions, Berlin 1979, Springer Verlag, Berlin.
- 6 J. Cugnon, C. Volant, S. Vuillier, *Nucl. Phys. A* **620** 475-496 (1997).
- 7 A.R. Junghans, M. de Jong, H.-G. Clerc, A.V. Ignatyuk, G.A. Kudyaev, K.-H. Schmidt, *Nucl. Phys. A* **629** 635-654 (1998).
- 8 J. Benlliure, A. Grewe, M. de Jong, K.-H. Schmidt, S. Zhdanov, *Nucl. Phys. A* **628** 458-469 (1998)
- 9 S.I. Mulgina, K.-H. Schmidt, A. Grewe, S.V. Zhdanov, *Nucl. Phys. A* **640** 375-387 (1998).
- 10 A.V. Ignatyuk, K. K. Istekov, G. N. Smirenkin, *Yad. Fiz.* **29** (1979) 875-883 (*Sov. J. Nucl. Phys.* **29** 450-454 (1979))
- 11 L. G. Moretto, G. Wozniak, "The Categorical Space of Fission", LBL-25744 (1988)